A Novel Method of Copula Connectivity-based and Collatz Patterns Schemes for Detection of Mild Cognitive Impairment and Alzheimer Patients using Magnetoencephalogram

Hadis Biglari [a,*], Mehran Yazdi [a], Mahsa Taghavi [b], Saeid Sanei [c], Reza Boostani [a]

a. School of Electrical and Computer Engineering, Shiraz University, Shiraz, Iran
b. Psychiatric Department, Medical School, Azad University, Kazerun Branch, Kazerun, Fars, Iran
c. Department of Electronic Engineering, Imperial College London, London, London, UK

* Corresponding author: hadis.biglari@hafez.shirazu.ac.ir

Keywords

Alzheimer;
Collatz Patterns;
Copula Function;
Brain Connectivity;
MEG;
Feature Fusion.

Abstract

Differentiating between Alzheimer's Disease (AD), Mild Cognitive Impairment (MCI), and healthy controls (HCs) remains a significant challenge in neuroscience. The existing methods based on electroencephalogram (EEG) or magnetoencephalogram (MEG) connectivity analysis, often focus on two-class classification and struggle to effectively capture both functional and causal brain connectivity for a three-class differentiation. To address this gap, we propose a novel multilevel connectivity scheme that integrates Copula theory and the Collatz pattern to estimate both linear and nonlinear connectivity levels between MEG channels. MEG signals from 62 participants (24 AD, 14 MCI, and 24 HC) were analyzed, with features combined using canonical correlation analysis (CCA) and refined through principal component analysis (PCA) and minimum redundancy maximum relevance (mRMR). This hybrid method, utilizing Frank Copula and Collatz pattern-based features, achieved a classification accuracy of 98.94% for three-class differentiation. The innovation stems from the ability of Copula features to capture both functional and causal relationships. When these features are combined with Collatz pattern features, the fusion approach outperforms the existing connectivity methods, including Granger causality. This approach provides a more accurate and comprehensive method for distinguishing between AD, MCI, and HC, filling a crucial gap in current neuroimaging research.

1. Introduction

By increasing age, people are more prone to age-related disorders, including cognitive decline and Alzheimer's disease (AD) as the most common cause of dementia [1]. The Alzheimer's Association estimates 6.9 million Americans will have AD in 2024; by 2025, this will rise to 12.7 million aged 65 years and above. The yearly rate at which mild cognitive impairment (MCI) progresses to AD is 8–15% [2], increasing to nearly one in four in low- and middle-income countries within 3–5.8 years [3]. Nonetheless, accurate differentiation between MCI and AD remains a challenge [4,5]. Several studies have addressed this using EEG. Due to head tis- sue transparency to magnetic fields, higher spatial resolution, and less intrusiveness, MEG analysis has attracted attention.

Despite being noisier than EEG, MEG is more accurate due to lower sensitivity to tissue properties and higher spatial resolution with many electrodes, though less accessible and costlier. A current challenge in AD diagnosis and MEG analysis lies in distinguishing AD, MCI, and healthy individuals, given the complex, nonlinear, and non-Gaussian nature of neural connectivity. Traditional methods rely on linear measures such as Pearson correlation or Granger causality, which may miss higher-order or asymmetric dependencies [6,7]. Moreover, most frameworks treat functional and effective connectivity separately, limiting holistic representation [6]. To address this, we propose a hybrid frame- work integrating two complementary feature strategies: Collatz sequence captures multi-level structural regularities in brain dynamics, and copula-based connectivity models non- linear dependencies across channels, including tail and asymmetric relations [8]. This yields a more discriminative representation, enabling detection of subtle network alterations in AD and MCI and improving classification compared to traditional methods [9].

A study by Lopez-Martin et al. introduced a deep learning model using MEG from MCI and AD subjects with randomized CNN, achieving high AD detection accuracy and presenting wavelet-based neuromarkers [10]. Another study found resting-state MEG useful for early AD discrimination [11]. In [12], Deep-MEG analyzed functional connectivity with image-based CNN ensembles. In [13], subject-specific FC- based frequency segmentation revealed MCI and AD network alterations. Yang et al. reconstructed source-space MEG using LCMV beamformer and wavelet-based neuromarkers for MCI detection [14]. In [15], tensors, CNN, and ResNet ap- plied to EEG achieved 100% MCI accuracy. These highlight MEG's potential for early AD detection. Due to its higher temporal resolution compared to imaging, MEG captures millisecond oscillations reflecting neural activity [1]. Neuronal activities are nonlinear (firing, thresholding, summation, saturation) [16], suiting nonlinear dynamical modeling. Non- linear coupling refers to intrinsic interactions modulated by extrinsic inputs, shaping overall cortical activity.

Functional connectivity (FC) is an effective representation of neural interactions [17] and a biomarker in neurodegenerative disease studies [18,19]. FC patterns provide insights into AD-related network disruptions [18]. Advanced AD affects FC, while hypersynchronization may be an early symptom. Resting-state studies show dual FC increases and decreases, especially in alpha band [20]. FC may be assessed by cross-correlation, assuming linearity and Gaussianity [21]. In [22], EEG signals were decomposed into IMFs with MEMD and classified using CNN. In [23], AEC- c showed sensitivity in beta band FC differences, while PLI was sensitive in theta globally but lacked regional precision. Granger causality (GC) has also proven promising for AD [24], revealing abnormal frequency-dependent MEG patterns [25]. Combining multiple measures with feature selection often

yields more effective results than correlation alone [26]. Integrating high-order dFC with traditional methods achieved improved MCI classification via SVM,surpassing earlier approaches [18]. In [27], nonlinear fMRI relation- ships in AD were modeled using kernel trick, achieving 98.68±0.79% accuracy.
To better reflect brain activity, nonlinear, non-Gaussian connectivity is crucial. Copula measures both linear and nonlinear dependencies regardless of Gaussianity [21]. Granger causality has been used to examine AD causality pattern changes [28-32]. We hypothesize Copula captures combined functional and nonlinear dependencies, improving brain connectivity estimation. In [21], Copula assessed FC in Parkinson's disease fMRI. Hence, for reliable AD and MCI discrimination, higher-order dependencies be- yond linear ones should be considered. Copula applied to AD EEG data [33] showed enhanced detection when combined with synchronization parameters. Signal decomposition also helps extract multi-level features. Maximum absolute pooling (MAP), halving signal length per level, and Collatz-based feature extraction, previously used in schizophrenia detection [34], employ a 4-level decomposition strategy. Such a hybrid approach is anticipated to improve AD and MCI identification [35].
Despite the promising results of previous studies, several limitations remain. Many existing connectivity measures assume linear or Gaussian interactions, which may fail to capture the nonlinear and asymmetric dependencies inherent in neurodegeneration. Most prior works rely on either connectivity measures or signal-based descriptors, neglecting complementary information from both intra-channel dynamics and inter-channel dependencies. Motivated by this, our work integrates two feature categories: Collatz features capture intra-channel temporal dynamics and structural regularities of MEG signals, while Copula-based measures quantify inter-channel dependencies, including complex non-linear and non-Gaussian relationships. Unlike traditional metrics such as PLV or MI, Copula offers a more flexible framework. Combining Collatz and Copula features thus provides a richer representation of local and global brain dynamics, beneficial for discriminating AD and MCI. Our main contribution is a novel feature engineering approach that jointly models brain signals. We are the first to fuse Frank Copula connectivity with Collatz patterns to capture both non-linear dependencies and dynamic complexity in 148-channel MEG data. This mathematically distinct combination improves discrimination in the challenging three-class problem. In the following sections, we explain our contributed approach, implemented in MATLAB R2023a, for classification of the above three groups.
The rest of this paper is organized as follow. Section 2 ex- plains the dataset used in this study then regions of brain on which the sensors are located, followed by the algorithms for estimation of Copula and Collatz features. Section 3 shows the achieved results and comparison with other methods. The last section concludes the paper.

2. Materials and Methods

The schematic diagram in Figure 1, provides an overview of the key components involved in the study. The diagram is divided into multiple blocks, each representing a significant stage in the method including MEG data recording, preprocessing, feature extraction, feature merging and selection, and classification. Each of these blocks is explained in more detail in subsequent sections to describe the rationale, methodology, and algorithms used at each stage.

2.1. Multichannel MEG

MEG signals were collected from 62 subjects, including 24 with AD, 14 with MCI, and 24 HC subjects [36]. The clinical diagnosis was based on extensive medical, neurological, psychiatric, neuroimaging (SPECT and MRI), and neuropsychological examinations. The AD group consisted of 6 males and 18 females aged 74.06 ± 6.95 years (mean ± standard deviation (Std)), while the MCI group consisted of 14 subjects (6 males and 8 females) aged 74.89 ± 5.57 years Finally, elderly control subjects have 8 males and 16 females aged within 71.77 ± 6.38 years also were included in this dataset. The signals were acquired by a 148 channel whole head magnetometer (MAGNES 2500 WH, 4D Neuroimaging).

2.2. Preprocessing

The denoising process involved visually selecting 17.25 ± 6.47 epochs of 10 seconds (1695 samples) with minimal ocular activity per subject using an expert's amplitude thresholding method, and removing cardiac artifacts using a con- strained blind source separation (cBSS) procedure. For each epoch the average of all MEG channels was used as a reference for cardiac activity rejection [36]. This makes the cardiac activity more pronounced compared to the background. Then cBSS is used to restore the MEG signals [37]. Channels were grouped into 8 regions as shown in Figure 2, using a mapping of the standard 148-channel MEG [38].

2.3. Feature extraction

2.3.1. Collatz feature extraction:

We used the Collatz conjecture-based approach proposed by Baygin et al. [34] for accurate schizophernia detection from EEG. This is the first time this feature generation approach are used for AD/MCI detection. The Collatz pattern is combined with a novel multilevel feature generating technique known as the maximal absolute pooling (MAP) decomposer to extract both low-level and high-level data. Because of extracting both low-level and high-level features for EEG applications, it has been indicated that the use of Collatz pattern improved the detection result.
MAP is a simple signal decomposition technique in which the signal length is halved at each level by retaining the element with the larger absolute value from each non-overlapping two-sample block [34]. This process yields multi-resolution representations of the original signal. The advantage of capturing both low-level and high-level features arises from this combination: MAP provides multi-level signal representations, while the Collatz algorithm extracts structural and nonlinear descriptors from each level. Together, they enable the proposed method to capture temporal dynamics at multiple scales. Below, one can see pseudocode of the used Collatz pattern [34], which is defined as CL(.) in Algorithm 1.
All parameters are chosen according to used parameters in [34] for EEG data. The steps of Collatz feature extraction are described in detail below:

Step 1: Divide each MEG channel into overlapping blocks of 16 samples. Let bl(i) denote the i_{th} sample within a given block.
Step 2: Apply two mathematical kernels to convert signals into binary arrays and generate bits using Eqs. (1)-(2):

$$krnl1(q,t)=\begin{cases}0, & q-t<0\\ 1, & q-t\geq 0\end{cases}, \tag{1}$$

$$krnl2(q,t)=\begin{cases}0, & q-t>0\vee |q|-|t|<0\\ 1, & q-t\leq 0\wedge |q|-|t|\geq 0\end{cases}, \tag{2}$$

The first and second kernels, krnl1(., .) and krnl2(., .) respectively, have parameters q and t. krnl1(., .) defines the signum function, which is a fundamental comparison function, and krnl2(., .) generates unsigned values.
Step 3: Extract 16 bits utilizing these kernels and the array Col = {6, 3, 10, 5, 16, 8, 4, 2, 1} using Eqs. (3)-(4). For a detailed description of how this array is constructed, please refer to Baygin et al. (2021) [34].

$$bit(j)=krnl1(bl(Col(j)),bl(Col(j+1))),\quad j\in\{1,2,\ldots,8\}, \tag{3}$$

$$bit(j+8)=krnl2(bl(Col(j)),bl(Col(j+1))),\quad j\in\{1,2,\ldots,8\}, \tag{4}$$

Step 4: Divide the retrieved segments into the f 1 and f 2 non- overlapping groups using Eqs. (5)-(6).

$$f1(j)=bit(j),\quad j\in\{1,2,\ldots,8\}, \tag{5}$$

$$f2(j)=bit(j+8),\quad j\in\{1,2,\ldots,8\}, \tag{6}$$

Step 5: In steps 3 and 4, pairs of consecutive samples from the 16-sample block bl(i:i+15), extracted in step 1, are passed to the binary kernels krnl1 and krnl2 to generate two 8-bit vectors. These binary values are then converted to decimal as follows (Eqs. (7)-(8)):

$$fm(i)=\sum_{j=1}^{8} f1(j)\cdot 2^{8-j},\quad i\in\{1,2,\ldots,M-15\}, \tag{7}$$

$$sm(i)=\sum_{j=1}^{8} f^{2}(j)\cdot 2^{8-j},\quad i\in\{1,2,\ldots,M-15\}, \tag{8}$$

where M describes the length of the MEG signal.
Step 6: Create fm and sm histograms hf and hs with a resolution of 256.
The equations mentioned earlier determine the starting value assignment of the histograms (hf and hs), and the process of creating them is discussed in Eqs. (9)-(10).

$$hf(fm(i))=hf(fm(i))+1, \tag{9}$$

$$hs(sm(i))=hs(sm(i))+1, \tag{10}$$

Step 7: To extract the final feature vector (fv), which has a length of 512, merge hf and hs (Eqs. (11)-(12)).

$$fv(l)=hf(l),\quad l\in\{1,2,\ldots,256\}, \tag{11}$$

$$fv(l+256)=hs(l),\quad l\in\{1,2,\ldots,256\}, \tag{12}$$

The Collatz-based features are computed independently for each MEG channel, without considering cross-channel dependencies. These features capture the local temporal dynamics within each channel by encoding short-term fluctuations into binary patterns and histograms. Consequently, they reflect intra-channel signal behavior rather than inter-channel functional connectivity. This temporal encoding enhances the discriminative power of the extracted features, particularly for detecting subtle signal variations associated with neurodegenerative conditions.
The final normalized features are depicted in Figure 3 for the same channel of three groups. This figure provides a visual comparison of how the normalized Collatz-based features vary between these groups, highlighting key distinctions in their brain connectivity patterns.

2.3.2. Copula feature extraction:

Assuming that the correlation between activities in various brain regions is linear and has a Gaussian structure, cross- correlation analysis is the most commonly employed method for investigating FC [34]. As this presumption might not be true for all cases, recently the researchers have tended to use other metrics in order to consider comprehensive dependencies as well. Copulas modeling can measure nonlinear relationships between time series [21]. Copula connects the marginal density functions using Copula density function in order to regain the joint density function, which implicitly illustrates the dependency among variables. Accordingly, the Copula model has been extensively utilized in the analysis of time series with significant dependency or complex dependence structures. Having complex dependence among different channels, the brain activities have motivated researchers to develop EEG-based [21,33,39] and fMRI-based Copula models [40,41].
Copula is a function that can completely describe the statis- tical dependency between random variables with arbitrary marginal distribution. To investigate nonlinear dependency between different regions,3 types of Copula functions including Gaussian, Student's t (also called t Copula), Clayton, Gumbel and Frank are used [21]. There are some methods to estimate marginal density functions and the correlation matrix parameters of the Copula density function and produce multivariate distribution. Among these methods, kernel density estimation (KDE) is more common. The marginal distributions are estimated using mixture KDE (MKDE) [39]. According to the literature, EEG-based Copula model is in its early stages and there is still potential progress to be made. Multivariate distribution between MEG signals are determined by combining univariate marginal distribution of each channel and Copula function family. In the other words, Copula functions are multivariate distributions while all univariate distributions are transformed to uniform distribution [42].

Let x1, ..., xN be the signal from N MEG channels with marginal cumulative distribution function (CDF) F1(x1), F2(x2), ..., FN (xN). Now, given these univariate marginal CDFs, the uniform distributions of the signals (u1, u2, ..., uN) can be assessed by using the probability integral transformation. According to Sklar's theorem [43], any multivariate joint distribution can be expressed by utilizing the individual univariate marginal distribution functions along with a Copula that characterizes the dependency among the variables. A Copula captures the dependence structure or correlation between variables in a multivariate distribution which are separated into the marginal distributions by transforming them to uniform distribution using probability integral transformation (Eq. (13)).

$$F(x1,\ldots,xN) = C(u1,u2,\ldots,uN), \tag{13}$$

Conversely, there is a unique Copula function which can re- construct the multivariate joint CDF F (x1, x2, ..., xN) (Eq. (14)).

$$F(X) = C-1[F(x1),F(x2),\ldots,F(xN)], \tag{14}$$

where C(.) is a Copula function and F (X) is joint CDF over all N observations. This dependence structure is assessed through two steps:

1) marginal distribution approximation of each MEG channel using MKDE,
2) estimation of Copula function parameters by maximum likelihood (ML) method.

For more clarity, let's do this for two MEG channels (x, y). In this case, N equals 2, and bivariate dependency is taken into account. The integral probability transformation was used to convert the data distribution to a uniform distribution. The uniform marginal distributions for these two ROI- time series are respectively U = (u1, u2, ..., uN) and V = (v1, v2, ..., vN) in [0, 1], as illustrated in Figure 4.

Each Copula function requires the estimation of its unknown parameters, θ, using techniques like ML estimation, by optimizing the log-likelihood function associated with the Copula family in order to best fit the joint CDF. In the following, three types of Copula functions that used in this paper along with their respective parameter ranges are listed in Eqs. (15)-(17):

1) Clayton Copula function

$$C(u,v\,|\,\theta) = (u^{-\theta}+v^{-\theta}-1)^{-1/\theta},\ \text{for}\ \theta\in(0,\infty), \tag{15}$$

where θ represents the tail dependence.

2) Frank Copula function

$$C(u,v|\ \theta) = \frac{1}{\theta}\log\left(1+\frac{(\exp(\theta u)-1)(\exp(\theta v)-1)}{\exp(\theta)-1}\right),\quad \theta\in[1,\infty), \tag{16}$$

where θ controls the tail dependence and affects the dependence structure.

3) Gumbel Copula function

$$C(u,v|\ \theta) = \exp\left\{-[(-\ln(u))^{\theta}+(-\ln(v))^{\theta}]^{1/\theta}\right\},\quad \theta\in[1,\infty), \tag{17}$$

In this Copula function, θ indicates the strength of the tail dependence.

Algorithm 1 Feature extraction & Classification
1: Input: 148 channels preprocessed MEG dataset
2: Output: Classification results
3: for S = 1, 2, . . . , N, S: segment do
4: for i, j = 1, 2, . . . , M, i,j: number of channels do
5: $\rho^{s}(i,j)$ = CPF (C)
6: where ρS is Copula parameter of each pair chan- nel, CPF (.) is Copula function, and C is the CDF of those pair channels
7: end for
8: fv^{s} = CL(MEG)
9: CL(.) is Collatz pattern feature generation
10: end for
11: Merge CPF and CL features using CCA method
12: Apply PCA and MRMR for feature selection
13: Use these classifiers (weighted KNN and multiclass SVM) and obtain classification results.

2.4. Feature fusion

Canonical correlation analysis (CCA) has emerged as a powerful and versatile technique for feature fusion, especially in multimodal contexts where data from different sources or feature extraction methods need to be integrated into a unified representation. CCA maximizes the correlation between two feature sets by projecting them into a shared latent space, capturing the most relevant and complementary information from both sets [44-46]. This ability to preserve the most informative aspects of different modalities makes CCA particularly suitable for complex tasks such as medical diagnosis and classification, where leveraging multiple feature sets can improve accuracy and robustness. In this study, we applied CCA to fuse features derived from the Copula and Collatz methods, two distinct approaches that capture different aspects of the underlying data. By using CCA, we combined the complementary information from these feature ex- traction techniques, enabling the creation of a richer, more informative feature space. This fused feature representation was then used for the recognition and classification of AD and MCI.

2.5. Feature selection

Due to the high number of channels, extracted features were highly dimensional, and zero-padding was needed to standardize inputs, introducing potential redundancy. To address this, we applied PCA to reduce dimensionality by capturing the most significant variance and mRMR to select features highly relevant to class labels (AD, MCI, HC) while minimizing redundancy. To prevent information leakage during model training and evaluation, all preprocessing steps, including normalization, dimensionality reduction via PCA, and feature ranking through mRMR, were strictly performed on the training data within each fold of the cross-validation process. These transformations were subsequently applied to the test data. This ensures that no information from the test fold influenced the training phase, and thus performance estimates remain unbiased. This ensured that the selected features provided diverse and informative representations, further improving classification performance. By combining PCA and mRMR, we effectively minimized overfitting and optimized the feature set, resulting in improved classification ac- curacy in the context of three-class classification The dimensionality of the feature sets at different stages of the pipeline is summarized as follows. For each subject, the Collatz method produced 2560 features (five sets of 512 features from the original signal and four MAP-decomposed levels). Copula-based connectivity yielded 72668 features by flattering the 148×148 matrices across temporal segments. The concatenated feature vector thus comprised 75228 dimensions. To reduce computational complexity and avoid overfitting, Principal Component Analysis (PCA) was applied, reducing the dimensionality to 114 while preserving over 95% of the variance.

Subsequently, the MRMR algorithm was employed for feature ranking. The same 114 features were retained, but reordered based on their discriminative importance.

2.6. Classification

For the merged Copula and Collatz features, an ANOVA test was conducted to determine whether the null hypothesis— that the three classes have the same mean—could be rejected. As shown in Figure 5, there is no overlap between the class means, indicating a statistically significant difference ($p < 0.001$).

In order to select the most effective classifier and groups of features for 3-way classification, we evaluated three types of Copula combined with Collatz features across the three classes. The classifiers are "weighted KNN" and "multiclass SVM" for 3-way classification. The classifier tuning parameters can be found in Table 1.

3. Results and Discussion

3.1. Experimental setup and results

In this section, we compare Copula and GC, and also pro- vided an overview of competitive methods such as mutual in- formation, PLV, GC, Collatz, and Copulas. Additionally, we discuss the classification results of these methods in comparison with the proposed approach.

3.1.1. Copula vs. Granger causality

As previously mentioned, the three types of Copula features employed measure the nonlinear joint probability of MEG channels and are used to assess joint connections. We com- pared these measures with GC to evaluate any pattern similarities. In Figure 6, some similarities between the Frank Copula and GC can be observed. Additionally, GC values were used for the classification of the three groups, with the results presented in Table 2. To standardize the GC values, we calculated the z-scores and then applied the same feature selection procedure to reduce redundancy and prevent over- fitting. (MI = Mutual Information, PLV = Phase Locking Value, GC = Granger Causality, Ent = Shannon entropy, Lyap = Lyapunov exponent, FD = Higuchi fractal dimension, Coll = Collatz, ClCop = Clayton Copula, FrCop = Frank Copula, GmCop = Gumbel Copula)

3.1.2. Comparison with other methods

The results are compared with both Collatz features and Cop- ula features individually. Furthermore, we employed two widely recognized synchronization measures, namely, phase locking value (PLV) and mutual information (MI), for com- parison. These metrics have gained significant attention in recent AD and MCI studies [47-50].

In references [51-58] recent 3-way classification methods compared with our method.

We compared classification results using weighted KNN and multiclass SVM. Weighted KNN modifies the standard KNN by assigning higher weights to closer neighbors and lower weights to farther ones, with classification based on weighted votes. The tuning parameters for some of the classifiers are listed in Table 1 and accuracy metric is used for validation of the performance. It should be noticed that the results are reported for 3-way classification (HC vs. MCI vs. AD) using these two classifiers with a 10-fold cross validation. The accuracy is calculated using Eq. (18):

$$Accuracy = \frac{TP + TN}{TP + TN + FN + FP} \times 100\%, \tag{18}$$

where TP, TN, FN and FP are true positives, true negative, false negatives, and false positives consecutively. In this study, multi-class accuracy was computed using a one-vs-all scheme and averaged across classes and folds, which is equivalent to calculating it directly from the multi-class confusion matrix.

3.1.3. Classification results

The 10-fold averaged results (HC vs. AD vs. MCI) using each classifier is shown in Figure 7. The overall classification results show that using the proposed connectivity estimation, AD, MCI, and HC can be classified with higher accuracy. As it can be seen in Table 2, the combination of Collatz patterns and Frank Copula (Coll + FrCop) outperformed all other combinations, achieving the highest accuracy for both SVM (98.94%) and KNN (98.69%). Multiclass ROC curves were also computed to evaluate classifier discrimination ability across folds (Figure 8 and Figure 9). It should be noted that some of the discrepancies observed between classifiers (e.g., the relatively different performance of GC features with KNN vs. SVM, or the variation in ClCop and

GmCop results) are mainly due to the limited sample size and the heterogeneous distribution of high-dimensional features, rather than implementation errors. This also explains the higher variance observed in certain cases.
The most recent studies are summarized in Table 3, where only a few address the classification of all three classes. The table compares datasets, methodologies, classifiers, and ac- curacies, reflecting recent progress in AD diagnosis using EEG and MEG. Many approaches rely on deep learning or feature extraction methods such as wavelet transforms, 2D images, and spectral topographical maps, often achieving high accuracy.
However, the proposed Frank Copula + Collatz approach surpasses them by integrating nonlinear connectivity measures with graph-based structural features. This shows that combining features reflecting multiple aspects of brain connectivity—probabilistic and topological—provides more accurate classification than one-dimensional or purely image-based features.
The proposed method achieves state-of-the-art accuracy and shows promise as a scalable, non-invasive diagnostic tool for detecting dementia-related brain changes. By surpassing complex deep learning models, it highlights that effective feature extraction and fusion can outperform data-hungry models, especially in medical applications with limited datasets.

3.2 Discussion

An important rationale behind the proposed framework lies in the complementary nature of the Collatz and Copula_based features. Collatz-derived descriptors are intra-channel measures that capture temporal dynamics and structural regularities within each individual MEG signal. They are effective in modeling non-linear patterns at the single-channel level but do not provide any information about cross-channel dependencies. In contrast, Copula-based connectivity features explicitly quantify inter-channel interactions and can model complex non-Gaussian, non-linear, and asymmetric dependencies across brain regions, yet they do not capture the intrinsic temporal structure of a single channel. By combining these two categories, the proposed approach simultaneously incorporates local dynamics (intra-channel) and global connectivity.
Regarding the choice of Copula over other connectivity metrics such as PLV or MI, it should be noted that these measures are mostly limited to linear or phase-synchronization relationships.
Copula, however, provides a more flexible framework capable of modeling both linear and higher-order nonlinear dependencies, as well as asymmetric relationships that are often overlooked by conventional methods. For this reason, Copula was selected as a more suitable complement to Collatz features, yielding a synergistic feature representation for MEG-based AD and MCI classification. Measurement of both linear and nonlinear FC estimates al- lowed us to capture both simple and complex patterns in the MEG signals more effectively. The hybrid methodology we employed—integrating Collatz pattern evaluation and Copula theory, demonstrated its effectiveness in discriminating between AD, MCI, and HC. The experimental results confirm that the proposed hybrid framework significantly outperforms conventional connectivity measures. Although Copula-based features alone yielded slightly lower performance than some traditional measures such as PLV or MI, their combination with Collatz descriptors resulted in a substantial improvement in classification accuracy. To the best of our knowledge, this is the first work to combine Collatz-derived features with Copula-based connectivity through a CCA-based fusion framework, followed by a two-stage feature selection (PCA and MRMR). This contribution enables a holistic representation of both local signal structure and global brain connectivity, thereby providing more discriminative power for distinguishing MCI and AD from healthy controls. Moreover, by reporting both mean and standard deviation across 10-fold cross-validation, as well as AUC values for both classifiers, the reliability and robustness of the proposed framework are demonstrated. These findings suggest that integrating intra-channel temporal dynamics with inter-channel connectivity is a promising direction for future MEG-based biomarker discovery in neurodegenerative diseases.
To ensure the robustness of our approach and avoid overfit- ting, we implemented strict cross-validation procedures using MATLAB's cvpartition function. All preprocessing steps, including normalization, PCA, and mRMR, were confined to the training data within each fold and applied to the test set subsequently. This protocol, along with the visualization of classification performance across folds (Figure 7), confirmed the reliability and fairness of our model evaluation process. To further support these findings, we computed multiclass ROC curves (see Figure 8 and Figure 9) across 10 folds for both SVM and KNN classifiers. Results showed that the SVM classifier achieved high AUC values across all three classes (HC: 1.00, AD: 0.97, MCI: 0.98), confirming the strength of the classifier beyond accuracy alone. KNN also demonstrated competitive performance (HC: 0.96, AD: 0.79, MCI: 0.82), validating its relevance despite lower average accuracy.
Our method outperformed existing techniques, achieving exceptional accuracy in distinguishing AD, MCI, and HC. The highest accuracy (98.94%) with multiclass SVM highlights the benefit of combining linear and nonlinear measures. The Frank Copula function effectively captured nonlinear dependencies between MEG channels, and when fused with Collatz patterns, significantly improved performance. Evaluated on 62 subjects (24 AD, 14 MCI, 24 HC) with 10-fold cross- validation, the hybrid approach consistently outperformed benchmarks (Table 2), with Collatz–Copula fusion yielding the best results. Comparison with established measures such as GC, MI, PLV, Lyapunov Exponents, FD, and Shannon Entropy (Table 3) confirmed its superiority in capturing subtle brain dynamics. A limitation is the small dataset size, and while rigorous statistical methods were applied, further validation on larger datasets is needed for broader clinical application.

4. Conclusions

In this study, we proposed a novel approach combining Collatz pattern generation with Copula connectivity for classifying AD, MCI, and HC subjects. Collatz patterns estimate intra-channel dynamics, while Copula captures non- linear inter-channel dependencies. Their integration lever- ages both local and global connectivity to improve classification. Comparative analyses with traditional complexity measures confirmed the superior discriminative power of the Collatz–Copula feature fusion. To further validate performance, multiclass ROC curves were generated using 10-fold cross-validation with a one-vs-all scheme. SVM showed near- perfect separation with AUCs of 0.9986 (HC), 0.9703 (AD), and 0.9839 (MCI). KNN also performed well,

with AUC = 0.958 for HC and slightly lower for MCI and AD. These values closely match the reported accuracies (98.94% SVM, 98.69% KNN), confirming the robustness of the proposed features and pipeline.
Our hybrid methodology achieved over 96% accuracy in distinguishing the three groups, outperforming other methods by incorporating multilevel nonlinear features. These results highlight the value of combining linear and nonlinear FC measures to boost classification accuracy. While promising, larger datasets are needed to confirm generalizability. This study lays the groundwork for improved, non-invasive neuroimaging techniques for dementia diagnosis.

Acknowledgments

The authors declare that no acknowledgments are applicable for this work.

Authors' Credit

Hadis Biglari
Conceptualization; Data curation; Formal analysis; Investigation; Methodology; Software; Validation; Visualization; Writing – Original draft; Writing – review & editing
Mehran Yazdi
Conceptualization; Investigation; Methodology; Supervision; Validation; review & editing
Mahsa Taghavi
Conceptualization; interpreting the results, review & editing
Saeid Sanei
Conceptualization; Investigation; Data Preparation; Resources; Supervision; Validation; review & editing
Reza Boostani
Conceptualization; Formal analysis; Investigation; Methodology; Project administration; Supervision; Validation; Visualization; Writing – review & editing

Funding

The authors declare that they have no known competing financial interests or personal relationships that could have appeared to influence the work reported in this paper.

Conflicts of interest

The authors declare that they have no known competing financial interests or personal relationships that could have appeared to influence the work reported in this paper.

References

1. Torres-Simon, L., Doval, S., Nebreda, A., et al. "Understanding brain function in vascular cognitive impairment and dementia with EEG and MEG: A systematic review", NeuroImage Clin., 35, p. 103040 (2022). https://doi.org/10.1016/j.nicl.2022.103040
2. Ilardi, C. R., Chieffi, S., Iachini, T., et al. "Neuropsychology of posteromedial parietal cortex and conversion factors from Mild Cognitive Impairment to Alzheimer's disease: systematic search and state-of-the-art review", Aging Clin. Exp. Res., 34(2), pp. 289–307 (2022). https://doi.org/10.1007/s40520-021-01930-y
3. McGrattan, A. M., Pakpahan, E., Siervo, M., et al. "Risk of conversion from mild cognitive impairment to dementia in low- and middle-income countries: A systematic review and meta-analysis", Alzheimer's & Dementia: Translational Research & Clinical Interventions, 8(1), p. e12267 (2022). https://doi.org/10.1002/trc2.12267
4. Yang, S., Bornot, J. M. S., Wong-Lin, K., et al. "M/EEG-based bio-markers to predict the MCI and Alzheimer's disease: a review from the ML perspective", IEEE Trans. Biomed. Eng., 66(10), pp. 2924–2935 (2019). https://doi.org/10.1109/TBME.2019.2898871
5. Biglari, H., Boostani, R., Yazdi, M., et al. "A New Minimum Spanning Tree based Analysis of EEG and MEG with Application to Classification of Alzheimer's Disease", IEEE Access (2025). https://doi.org/10.1109/ACCESS.2025.3585196
6. Friston, K. J. "Functional and effective connectivity: a review", Brain Connect., 1(1), pp. 13–36 (2011). https://doi.org/10.1089/brain.2011.0008
7. Herzog, R., Rosas, F. E., Whelan, R., et al. "Genuine high-order interactions in brain networks and neurodegeneration", Neurobiol. Dis., 175, p. 105918 (2022). https://doi.org/10.1016/j.nbd.2022.105918
8. Mesiar, R. and Sheikhi, A. "Nonlinear random forest classification, a copula-based approach", Appl. Sci., 11(15), p. 7140 (2021). https://doi.org/10.3390/app11157140

9. Akbar, F., Taj, I., Usman, S. M., et al. “Unlocking the potential of EEG in Alzheimer's disease research: Current status and pathways to precision detection”, Brain Res. Bull., 223, p. 111281 (2025). https://doi.org/10.1016/j.brainresbull.2025.111281

10. Lopez-Martin, M., Nevado, A., and Carro, B. “Detection of early stages of Alzheimer's disease based on MEG activity with a randomized convolutional neural network”, Artif. Intell. Med., 107, p. 101924 (2020). https://doi.org/10.1016/j.artmed.2020.101924

11. Saleem, T. J., Zahra, S. R., Wu, F., et al. “Deep learning-based diagnosis of Alzheimer's disease”, J. Pers. Med., 12(5), p. 815 (2022). https://doi.org/10.3390/jpm12050815

12. Giovannetti, A., Susi, G., Casti, P., et al. “Deep-MEG: spatiotemporal CNN features and multiband ensemble classification for predicting the early signs of Alzheimer's disease with magnetoencephalography”, Neural Comput. Appl., 33(21), pp. 14651–14667 (2021). https://doi.org/10.1007/s00521-021-06105-4

13. Rodríguez-González, V., Núñez, P., Gómez, C., et al. “Unveiling the alterations in the frequency-dependent connectivity structure of MEG signals in mild cognitive impairment and Alzheimer's disease”, Biomed. Signal Process. Control, 87, p. 105512 (2024). https://doi.org/10.1016/j.bspc.2023.105512

14. Yang, S., Bornot, J. M. S., Fernandez, R. B., et al. “Detection of mild cognitive impairment with MEG functional connectivity using wavelet-based neuromarkers”, Sensors, 21(18), p. 6210 (2021). https://doi.org/10.3390/s21186210

15. Şeker, M. and Özerdem, M. S. “Deep insights into MCI diagnosis: A comparative deep learning analysis of EEG time series”, J. Neurosci. Methods, 403, p. 110057 (2024). https://doi.org/10.1016/j.jneumeth.2024.110057

16. Sanei, S. and Chambers, J. A. EEG Signal Processing and Machine Learning. John Wiley & Sons (2021). https://doi.org/10.1002/9781119386957

17. Modares-Haghighi, P., Boostani, R., Nami, M., et al. “Quantification of pain severity using EEG-based functional connectivity”, Biomed. Signal Process. Control, 69, p. 102840 (2021). https://doi.org/10.1016/j.bspc.2021.102840

18. Filippi, M., Spinelli, E. G., Cividini, C., et al. “Resting state dynamic functional connectivity in neurodegenerative conditions: a review of magnetic resonance imaging findings”, Front. Neurosci., 13, p. 657 (2019). https://doi.org/10.3389/fnins.2019.00657

19. Tóth, B., File, B., Boha, R., et al. “EEG network connectivity changes in mild cognitive impairment—Preliminary results”, Int. J. Psychophysiol., 92(1), pp. 1–7 (2014). https://doi.org/10.1016/j.ijpsycho.2014.02.001

20. Maestú, F., Cuesta, P., Hasan, O., et al. “The importance of the validation of M/EEG with current biomarkers in Alzheimer's disease”, Front. Hum. Neurosci., 13, p. 17 (2019). https://doi.org/10.3389/fnhum.2019.00017

21. Ghasemi, M., Zarei, M., Foroutannia, A., et al. “Study of functional connectivity of central motor system in Parkinson's disease using copula theory”, Biomed. Signal Process. Control, 65, p. 102320 (2021). https://doi.org/10.1016/j.bspc.2020.102320

22. Jia, H., Huang, Z., Caiafa, C. F., et al. “Assessing the potential of data augmentation in EEG functional connectivity for early detection of Alzheimer's disease”, Cognit. Comput., 16(1), pp. 229–242 (2024). https://doi.org/10.1007/s12559-023-10188-7

23. Schoonhoven, D. N., Briels, C. T., Hillebrand, A., et al. “Sensitive and reproducible MEG resting-state metrics of functional connectivity in Alzheimer's disease”, Alzheimers. Res. Ther., 14(1), p. 38 (2022). https://doi.org/10.1186/s13195-022-00970-4

24. Juan-Cruz, C., Gómez, C., Poza, J., et al. “Assessment of effective connectivity in Alzheimer's disease using Granger causality”, in Converging Clinical and Engineering Research on Neurorehabilitation II, Springer, pp. 763–767 (2016). https://doi.org/10.1007/978-3-319-46669-9_125

25. Juan-Cruz, C., Gómez, C., Poza, J., et al. “Analysis of magnetoencephalography signals from Alzheimer's disease patients using granger causality”, 2016 38th Annu. Int. Conf. IEEE Eng. Med. Biol. Soc., IEEE, pp. 724–727 (2016). https://doi.org/10.1109/EMBC.2016.7590804

26. Mohanty, R., Sethares, W. A., Nair, V. A., et al. “Rethinking measures of functional connectivity via feature extraction”, Sci. Rep., 10(1), p. 1298 (2020). https://doi.org/10.1038/s41598-020-57915-w

27. Ahmadi, H., Fatemizadeh, E., and Nasrabadi, A. “Investigation of non-linear functional connectivity in Alzheimer's disease utilizing resting state fMRI data and graph theory”, Iran. J. Biomed. Eng., 14(3), pp. 235–249 (2020). https://doi.org/10.22041/IJBME.2020.128322.1598

28. Sun, M., Xie, H., and Tang, Y. “Directed network defects in Alzheimer's disease using granger causality and graph theory”, Curr. Alzheimer Res., 17(10), pp. 939–947 (2020). https://doi.org/10.2174/1567205017666201215140625

29. Wang, M., Liao, Z., Mao, D., et al. “Application of Granger causality analysis of the directed functional connection in Alzheimer's disease and mild cognitive impairment”, J. Vis. Exp. JoVE, (126), p. 56015 (2017). https://doi.org/10.3791/56015

30. Wu, Y., Zhou, Y., and Song, M. “Classification of patients with AD from healthy controls using entropy-based measures of causality brain networks”, J. Neurosci. Methods, 361, p. 109265 (2021). https://doi.org/10.1016/j.jneumeth.2021.109265

31. Su, R., Yin, B., Jing, J., et al. “Information segregation and integration of aMCI based on genuine symbolic nonlinear Granger causality brain network”, Biomed. Signal Process. Control, 95, p. 106314 (2024). https://doi.org/10.1016/j.bspc.2024.106314

32. Hu, Y., Wen, C., Cao, G., et al. “Brain network connectivity feature extraction using deep learning for Alzheimer's disease classification”, Neurosci. Lett., 782, p. 136673 (2022). https://doi.org/10.1016/j.neulet.2022.136673

33. Iyengar, S. G., Dauwels, J., Varshney, P. K., et al. “Quantifying EEG synchrony using copulas”, 2010 IEEE Int. Conf. Acoust. Speech Signal Process., IEEE, pp. 505–508 (2010). https://doi.org/10.1109/ICASSP.2010.5495664

34. Baygin, M., Yaman, O., Tuncer, T., et al. “Automated accurate schizophrenia detection system using Collatz pattern technique with EEG signals”, Biomed. Signal Process. Control, 70, p. 102936 (2021). https://doi.org/10.1016/j.bspc.2021.102936

35. Hauk, O. “Source Estimation, Connectivity, and Pattern Analysis of EEG/MEG Data in Psycholinguistics”, in The Oxford Handbook of Psycholinguistics, Oxford University Press (2018). https://doi.org/10.1093/oxfordhb/9780198786825.013.41

36. Escudero, J., Sanei, S., Jarchi, D., et al. “Regional coherence evaluation in mild cognitive impairment and Alzheimer's disease based on adaptively extracted magnetoencephalogram rhythms”, Physiol. Meas., 32(8), pp. 1163–1180 (2011). https://doi.org/10.1088/0967-3334/32/8/011

37. Escudero, J., Hornero, R., Abásolo, D., et al. “Quantitative evaluation of artifact removal in real magnetoencephalogram signals with blind source separation”, Ann. Biomed. Eng., 39(8), pp. 2274–2286 (2011). https://doi.org/10.1007/s10439-011-0320-7

38. Fell, J., Röschke, J., Grözinger, M., et al. “Alterations of continuous MEG measures during mental activities”, Neuropsychobiology, 42(2), pp. 99–106 (2000). https://doi.org/10.1159/000026679

39. Zheng, Y., Zhao, X., and Yao, L. “Mixture kernel density estimation and remedied correlation matrix on the EEG-based copula model for the assessment of visual discomfort”, Cognit. Comput., 12(6), pp. 1130–1143 (2020). https://doi.org/10.1007/s12559-020-09771-3

40. Lee, N. and Kim, J. “Copula directional dependence for inference and statistical analysis of whole-brain connectivity from fMRI data”, Brain Behav., 9(1), p. e01191 (2019). https://doi.org/10.1002/brb3.1191

41. Ince, R. A. A., Giordano, B. L., Kayser, C., et al. “A statistical framework for neuroimaging data analysis based on mutual information estimated via a gaussian copula”, Hum. Brain Mapp., 38(3), pp. 1541–1573 (2017). https://doi.org/10.1002/hbm.23471

42. Silva, R. dos S. and Lopes, H. F. “Copula, marginal distributions and model selection: a Bayesian note”, Stat. Comput., 18(3), pp. 313–320 (2008). https://doi.org/10.1007/s11222-008-9058-y

43. Durante, F. and Sempi, C. Principles of Copula Theory. CRC Press, Boca Raton, FL (2016). Print ISBN: 9781439884423; eBook ISBN: 9781439884447.

44. Sarvestani, R. R. and Boostani, R. “FF-SKPCCA: Kernel probabilistic canonical correlation analysis”, Appl. Intell., 46(2), pp. 438–454 (2017). https://doi.org/10.1007/s10489-016-0854-9

45. Jia, H., Wang, Y., Duan, Y., et al. “Alzheimer's disease classification based on image transformation and features fusion”, Comput. Math. Methods Med., 2021(1), p. 9624269 (2021). https://doi.org/10.1155/2021/9624269

46. Wei, K., Kong, W., and Wang, S. “An improved multi-task sparse canonical correlation analysis of imaging genetics for detecting biomarkers of Alzheimer's disease”, IEEE Access, 9, pp. 30528–30538 (2021). https://doi.org/10.1109/ACCESS.2021.3059550

47. Rajji, T. “363. Theta-Gamma Coupling and Working Memory in Alzheimer′ s Dementia and Mild Cognitive Impairment”, Biol. Psychiatry, 81(10), pp. S148–S149 (2017). https://doi.org/10.1016/j.biopsych.2017.02.1153

48. Gaubert, S., Raimondo, F., Houot, M., et al. “EEG evidence of compensatory mechanisms in preclinical Alzheimer's disease”, Brain, 142(7), pp. 2096–2112 (2019). https://doi.org/10.1093/brain/awz150

49. Nimmy, J. T., Subha, D. P., and Menon, R. N. “Mutual information analysis on MCI-AD EEG signal during resting and task conditions”, TENCON 2019-2019 IEEE Reg. 10 Conf., IEEE, pp. 2295–2299 (2019). https://doi.org/10.1109/TENCON.2019.8929363

50. Gupta, Y., Lee, K. H., Lee, J. J., et al. “Classification of Alzheimer's disease and mild cognitive impairment by pattern recognition of EEG power and coherence”, 2010 IEEE Int. Conf. Acoust. Speech Signal Process., IEEE (2010). https://doi.org/10.1109/ICASSP.2010.5495193

51. Poza, J., Gómez, C., García, M., et al. “Analysis of neural dynamics in mild cognitive impairment and Alzheimer's disease using wavelet turbulence”, J. Neural Eng., 11(2), p. 26010 (2014). https://doi.org/10.1088/1741-2560/11/2/026010

52. Jiao, B., Li, R., Tang, B., et al. “EEG-based neural biomarker for diagnosis and assessment of mild cognitive impairment and Alzheimer's disease”, Alzheimer's Dement., 19, p. e075957 (2023). https://doi.org/10.1002/alz.075957

53. Fouladi, S., Safaei, A. A., Mammone, N., et al. “Efficient deep neural networks for classification of Alzheimer's disease and mild cognitive impairment from scalp EEG recordings”, Cognit. Comput., 14(4), pp. 1247–1268 (2022). https://doi.org/10.1007/s12559-022-10033-3

54. Ieracitano, C., Mammone, N., Bramanti, A., et al. “A convolutional neural network approach for classification of dementia stages based on 2D-spectral representation of EEG recordings”, Neurocomputing, 323, pp. 96–107 (2019). https://doi.org/10.1016/j.neucom.2018.09.085

55. Ieracitano, C., Mammone, N., Hussain, A., et al. “A novel multi-modal machine learning based approach for automatic classification of EEG recordings in dementia”, Neural Networks, 123, pp. 176–190 (2020). https://doi.org/10.1016/j.neunet.2019.12.006

56. Bi, X. and Wang, H. “Early Alzheimer's disease diagnosis based on EEG spectral images using deep learning”, Neural Networks, 114, pp. 119–135 (2019). https://doi.org/10.1016/j.neunet.2019.02.005

57. Xia, W., Zhang, R., Zhang, X., et al. “A novel method for diagnosing Alzheimer's disease using deep pyramid CNN based on EEG signals”, Heliyon, 9(4) (2023). https://doi.org/10.1016/j.heliyon.2023.e14858

58. Rezaee, K. and Zhu, M. “Diagnose Alzheimer's disease and mild cognitive impairment using deep CascadeNet and handcrafted features from EEG signals”, Biomed. Signal Process. Control, 99, p. 106895 (2025). https://doi.org/10.1016/j.bspc.2024.106895

Figure and Table captions:

Figure 1. The schematic diagram of the proposed algorithm based on Copula and Collatz features for MCI and AD detection.

Figure 2. Eight human scalp regions and distribution of MEG electrodes on these regions, taken from [36]. The lines are boundaries between regions. Mid-line sensors are excluded.

Figure 3. Normalized Collatz features for the same channel of three groups.

Figure 4. (a) Marginal distributions and scatter plots of two MEG channels from different regions; (b) uniform distribution transformation.

Figure 5. ANOVA test result for Collatz-Frank Copula features of HC, MCI and AD with standard deviations of 0.18, 0.24 and 0.18 respectively from right to left. Groups 0 and 2 have means significantly different from group 1.

Figure 6. Frank Copula parameter patterns, Granger causality, and mutual information for AD, HC and MCI ($p < 0.05$).

FIGURE 7. 10-fold classification results for multiclass SVM and weighted KNN.

FIGURE 8. Multiclass ROC curves for the SVM classifier based on 10-fold cross-validation using the one-vs-all strategy. AUC values: HC = 0.9986, AD = 0.9703, MCI = 0.9839.

FIGURE 9. Multiclass ROC curves for the KNN classifier based on 10-fold cross-validation using the one-vs-all strategy. AUC values: HC = 0.958, AD = 0.7888, MCI = 0.8185.

Table 1. Tuning parameters for the used classifier.

Table 2. Comparison of 3-way classification accuracy of the proposed method using different features with KNN and SVM classifiers in terms of mean ± standard deviation.

Table 3. Comparison of 3-way classification accuracy.

Figures and Tables:

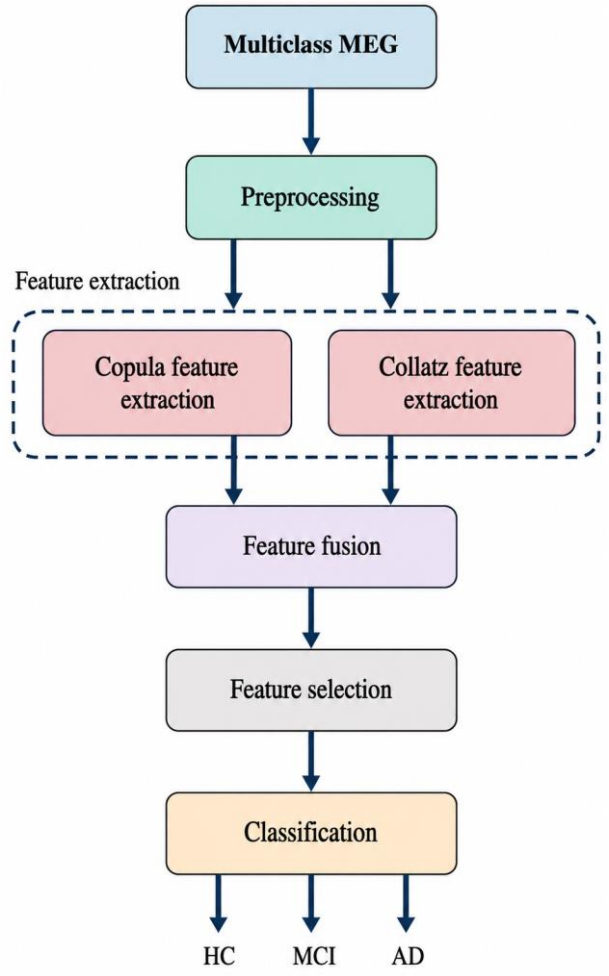

Figure 1.

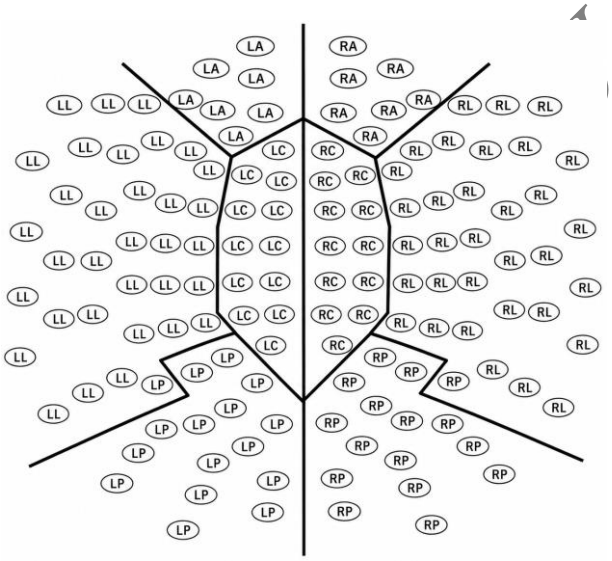

Figure 2.

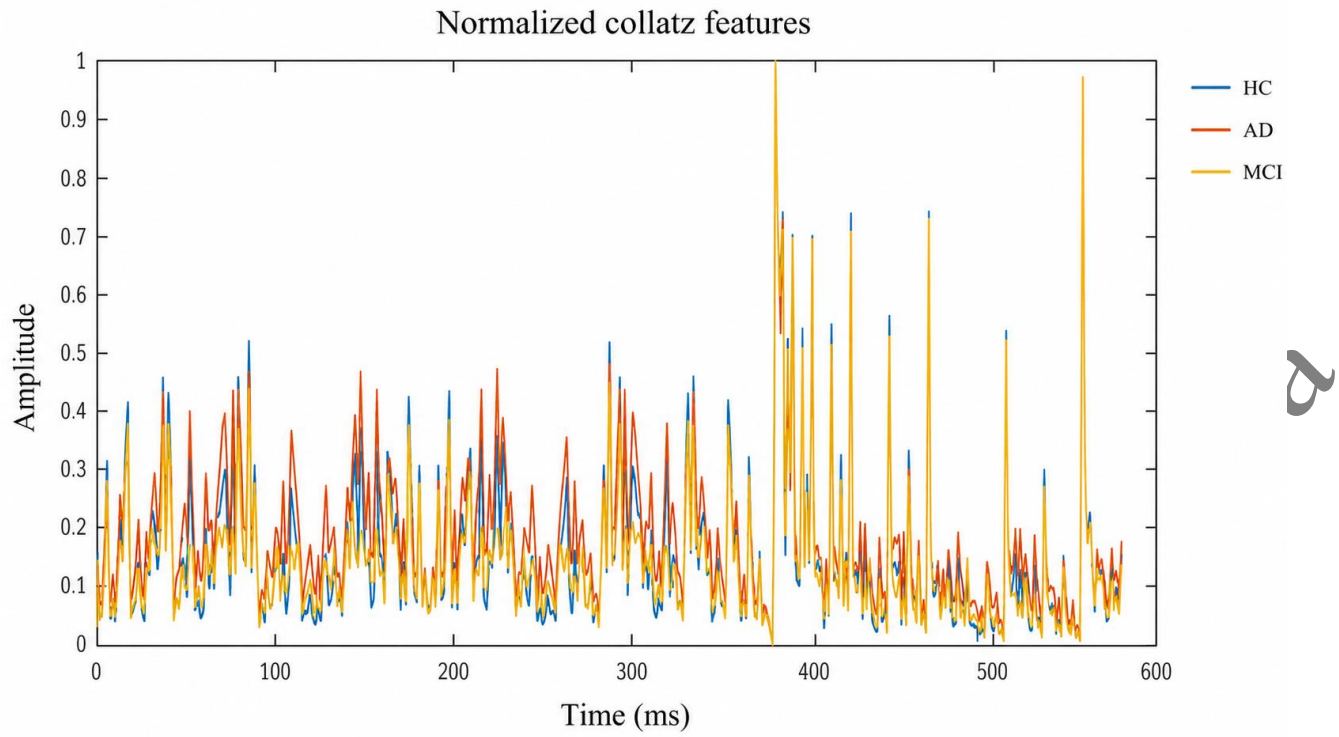

Figure 3.

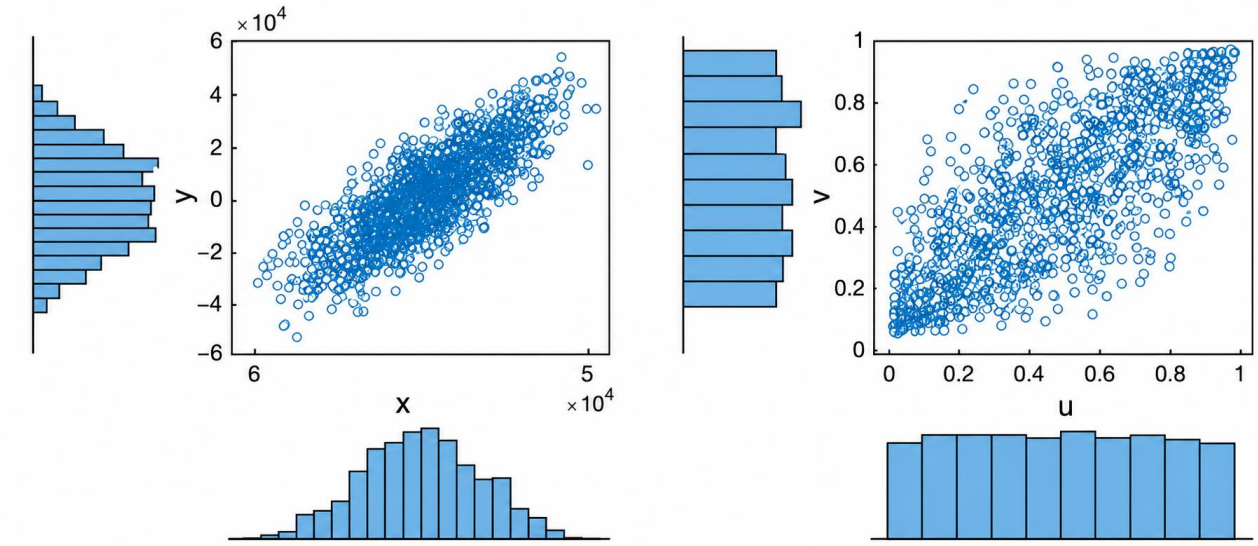

Figure 4.

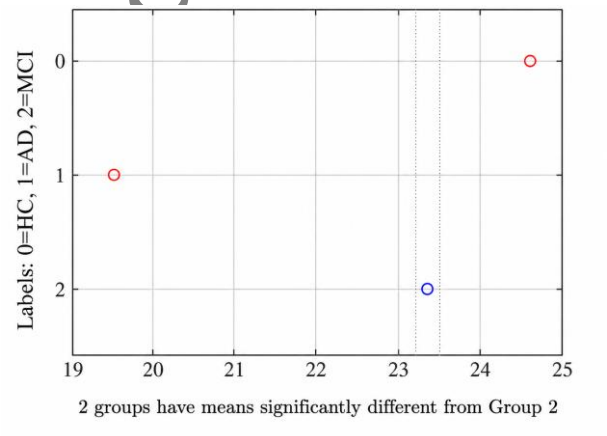

Figure 5.

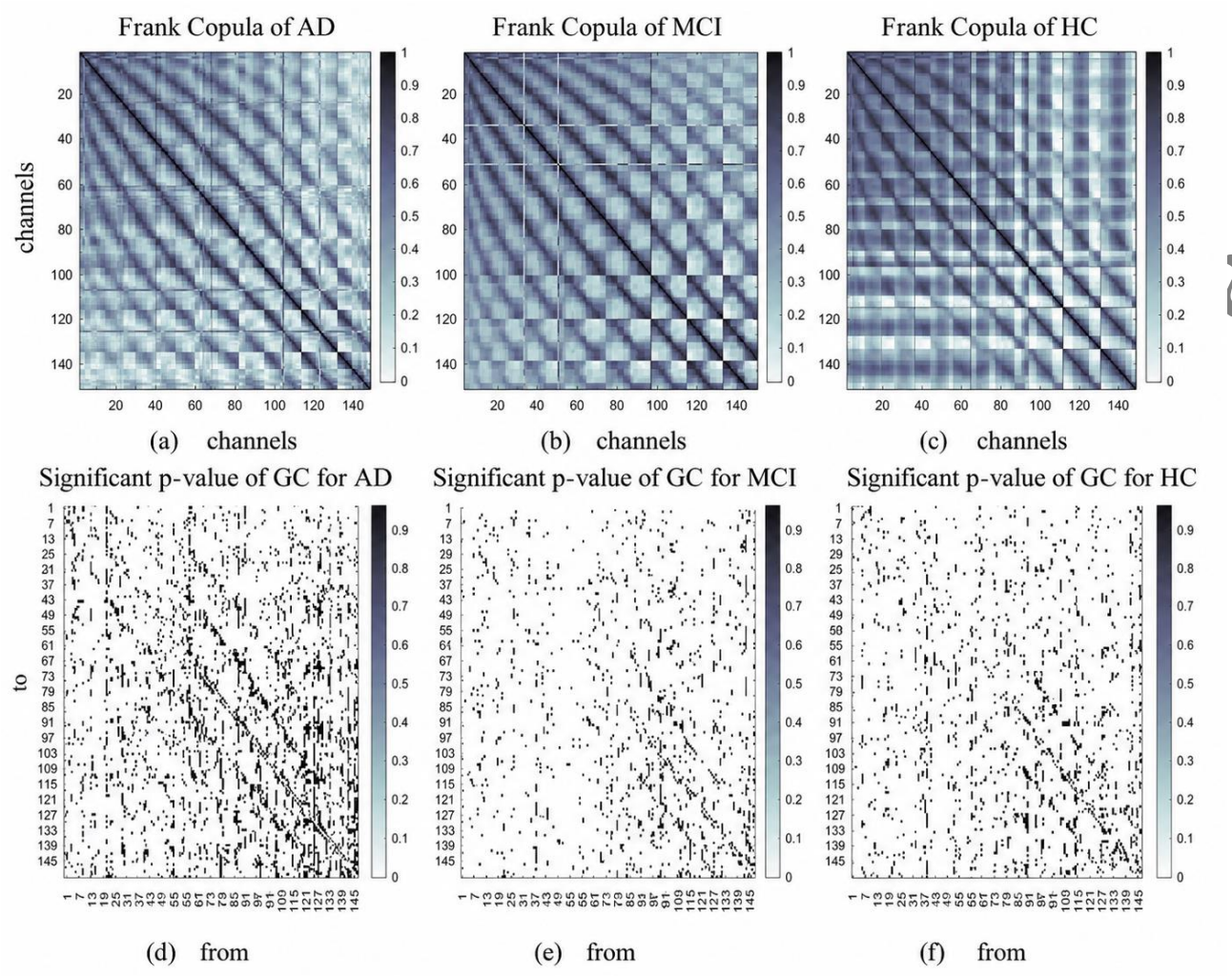

Figure 6.

Table 1.

Classifier	Parameters
weighted KNN	k = 10, Distance metric = Cosine distance weight = Squared inverse
SVM	Standardize = true, posterior estimation = enabled

KNN = k-Nearest Neighbors; SVM = Support Vector Machine.

Table 2.

Methodology	SVM (%)	KNN (%)
MI	95.33 ± 0.62	94.49 ± 0.77
PLV	71.24 ± 1.62	85±1.09
Gc	71.08 ± 1.35	45.31 ±0.81
Ent	71.15 ± 1.58	80.46±1.27
Lyap	70.97 ± 1.34	80.19±1.17
FD	68.21 ± 1.53	81.99±0.99
Coll	89.65 ± 0.44	90.98 ±1.6
ClCop	54.64 ± 0.71	72.88 ±1.08
GmCop	53.22 ± 0.56	74.11 ±1.21
FrCop	65.7 ± 0.92	94.52 ±0.87
Coll+ClCop	98.11 ± 2.21	96.86 ±1.63
Coll+GmCop	97.42 ± 1.02	96.33 ±1.85
Coll+FrCop	98.94 ± 2.07	98.69±1.52

MI = Mutual Information; PLV = Phase Locking Value; Gc = Granger Causality; Ent = Entropy; Lyap = Lyapunov Exponent; FD = Fractal Dimension; Coll = Coherence; ClCop, GmCop, and

FrCop denote coherence measures in the classical, gamma, and frontal frequency/regional bands, respectively; "+" indicates feature combination. All values are reported as mean ± standard deviation (%) across multiple runs.

Table 3.

Reference	Dataset	Methodology	Classifier	Results (%)
[52]	MEG (AD/MCI/HC)	Wavelet turbulence	Receiver operating characteristic (ROC) analysis	67.9
[53]	16-channel EEG (AD/MCI/other dementias/HC)	Combination of EEG + CSF + APOE measures	Random forest regressions	70
[54]	EEG (AD/MCI/HC)	2D RGB images from Mexican Hat = Continuous wavelet trans- form (CWT)	CNN Two hidden layers	82
[55]	19-channel EEG (AD/MCI/HC)	2D greyscale Periodogram images	Convolutional neural network (CNN) One hidden layer	83.3
[56]	19-channel EEG (AD/MCI/HC)	Features from Mexican Hat CWT and Bispectrum estimation	Multi-Layer Perceptron (MLP)	89
[57]	EEG (AD/MCI/HC)	2D RGB images by combining spectral topographical maps	Discriminative contractive slab and spike convolutional deep Boltzmann machine (DCss-CDBM)	95
[58]	19-channel EEG (AD/MCI/HC)	Frequency domain features	Deep pyramid convolutional neural network (DPCNN)	97.10
[59]	EEG (AD/MCI/HC)	Discrete wavelet transform (DWT)	CascadeNet model	98.84
Proposed method	148-channel MEG (AD/MCI/HC)	Combination of Frank Copula and Collatz	Multiclass SVM	98.94
[52]	MEG (AD/MCI/HC)	Wavelet turbulence	Receiver operating characteristic (ROC) analysis	67.9
[53]	16-channel EEG (AD/MCI/other dementias/HC)	Combination of EEG + CSF + APOE measures	Random forest regressions	70
[54]	EEG (AD/MCI/HC)	2D RGB images from Mexican Hat = Continuous wavelet trans- form (CWT)	CNN Two hidden layers	82

EEG = Electroencephalography; MEG = Magnetoencephalography; AD = Alzheimer's disease; MCI = Mild cognitive impairment; HC = Healthy control; CSF = Cerebrospinal fluid; APOE = Apolipoprotein E; ROC = Receiver operating characteristic; CWT = Continuous wavelet transform; CNN = Convolutional neural network; MLP = Multi-layer perceptron; DWT = Discrete wavelet transform; DPCNN = Deep pyramid convolutional neural network; SVM = Support vector machine. All values represent classification accuracy (%).

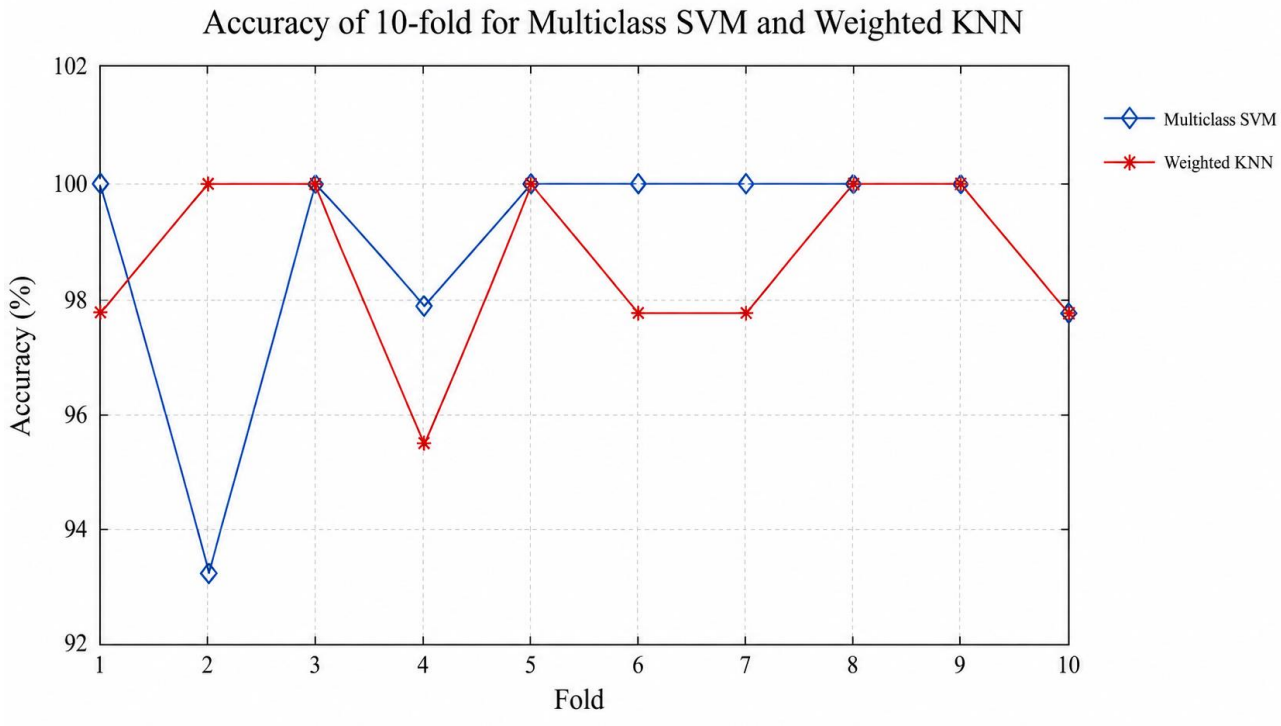

Figure 7.

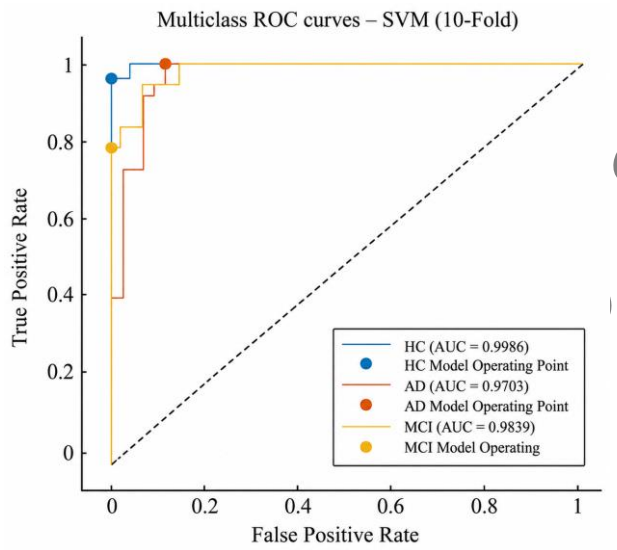

Figure 8.

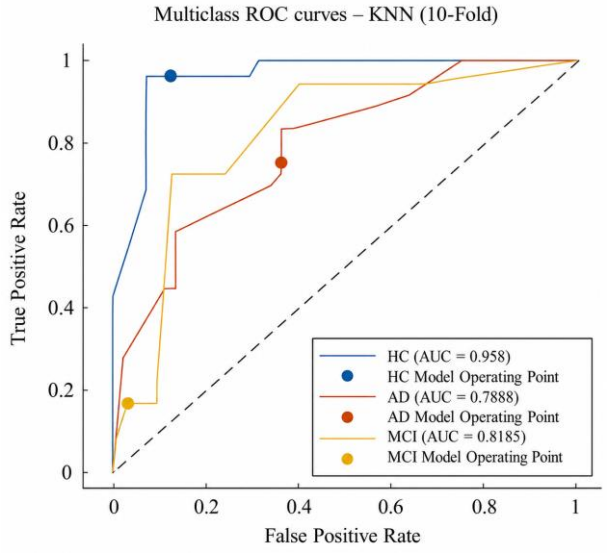

Figure 9.

Biographies

Hadis Biglari received the B.S. degree in electrical engineering from Islamic Azad University, Kermanshah, Iran, in 2012, and the M.S. degree in biomedical engineering from Shiraz University, Shiraz, Iran, in 2016. She is currently pursuing the Ph.D. degree in biomedical engineering at Shiraz University. Since 2021, she has been a Research and Development Specialist and Product Owner at ParsJahd Green Technologies, Tehran, Iran. Her research interests include biosignal processing, Alzheimer's disease, and machine learning techniques for medical health monitoring and wearable devices.

Mehran Yazdi received the B.Sc. degree in communication systems from Shiraz University, Shiraz, Iran, in 1992, and the M.Sc. and Ph.D. degrees in digital vision and image processing from Laval University, Quebec, QC, Canada, in 1996 and 2003, respectively. He is currently a Full Professor at Shiraz University. He has conducted several projects in video object tracking, CT metal artifact reduction, and medical signal processing, and has completed sabbatical periods at the Universities of Trois-Rivières (Canada) and La Rochelle (France).

Mahsa Taghavi received her General Practitioner (GP) degree from Kashan University of Medical Sciences in 2001 and her specialty board in Psychiatry from Shiraz University of Medical Sciences in 2006. She is currently a faculty member at Azad University of Kazerun, Iran. Her research interests focus on the diagnosis of psychiatric diseases through the analysis of EEG signals.

Saeid Sanei is a Fellow of the British Computer Society (FBCS) and received his Ph.D. from Imperial College London, UK. He has authored five books and over 450 peer-reviewed journal and conference papers. He has served as an Associate Editor for the IEEE Signal Processing Letters, IEEE Signal Processing Magazine, and Journal of Computational Intelligence and Neuroscience. He chaired IEEE ICASSP 2019 in Brighton, UK, and is currently a Visiting Academic in digital health at Imperial College London.

Reza Boostani received the B.Sc. degree in Electrical Engineering from Shiraz University in 1996, and the M.Sc. and Ph.D. degrees in Biomedical Engineering from AmirKabir University of Technology, Tehran, Iran, in 1999 and 2005, respectively. He is currently a Full Professor and the Head of the Biomedical Engineering Group at Shiraz University. He has been a distinguished researcher of the university in 2010, 2017, and 2022, and was listed among the top 2% highly cited researchers worldwide in 2022 and 2023. His research interests include biomedical signal processing, pattern recognition, and deep learning.